Electronic Supplementary Material (ESI) for Journal of Materials Chemistry C.

"Effect of aliovalent doping on properties of perovskite-like multiferroic formates"

by M. Mączka et al.

Table S1. Phase transition temperatures during heating and cooling as well as the observed changes in enthalpy ΔH and entropy ΔS of the studied compounds.

compound	T_c during heating K	T_c during cooling K	ΔH $KJmol^{-1}$	ΔS $Jmol^{-1}K^{-1}$
DMMn	190	182	0.898	4.7
DMMn: 2.1 % Cr^{3+}	177	172	0.327	1.9
DMMn: 3.1 % Cr^{3+}	158	152	0.168	1.1
DMMn: 2.0 % Al^{3+}	177	171	0.399	2.3
DMMn: 3.5 % In^{3+}	158	152	0.085	0.54
DMMn: 1.4 % Eu^{3+}	183	177	0.532	3.1
DMMn: 2.6 % Er^{3+}	159	152	0.096	0.6
DMMg	265	259	1.553	5.9
DMMg: 0.8 % Cr^{3+}	262	254	1.432	5.5
DMMg: 2.2 % Cr^{3+}	255	248	1.392	5.7
DMCo	159	149	0.551	3.4
DMCo: 1.4 % Cr^{3+}	141	134	0.108	0.77

Table S2. Peaks observed in DMMn: 3.1% Cr^{3+} emission recorded at 5 K with their tentative assignments.

Energy	Rel. Int.	Label
cm^{-1}	%	
14634.9	22	R2
14593.9	100	R1
14573.0	29	L($HCOO^-$)
14482.4	10	L($HCOO^-$)
14446.9	11	L($HCOO^-$)
14414.7	19	L($HCOO^-$)
14381.0	47	T'(Mn^{2+}) and T'($HCOO^-$)
14341.8	37	T'(Mn^{2+}) and T'($HCOO^-$)
14296.2	51	T'(Mn^{2+})
14209.5	10	T'(Mn^{2+}) and T'(Cr^{3+})
14168.5	34	T'(Mn^{2+}) and T'(Cr^{3+})
13814.2	3	ν_3($HCOO^-$)
13768.3	8	ν_3($HCOO^-$)
13568.4	1	ν_6($HCOO^-$) and ν_{as}(CNC)
13527.8	2	ν_6($HCOO^-$)
13304.5	3	ν_2($HCOO^-$)
13268.1	9	ν_2($HCOO^-$)

13214.6 2 $\nu_5(HCOO^-)$

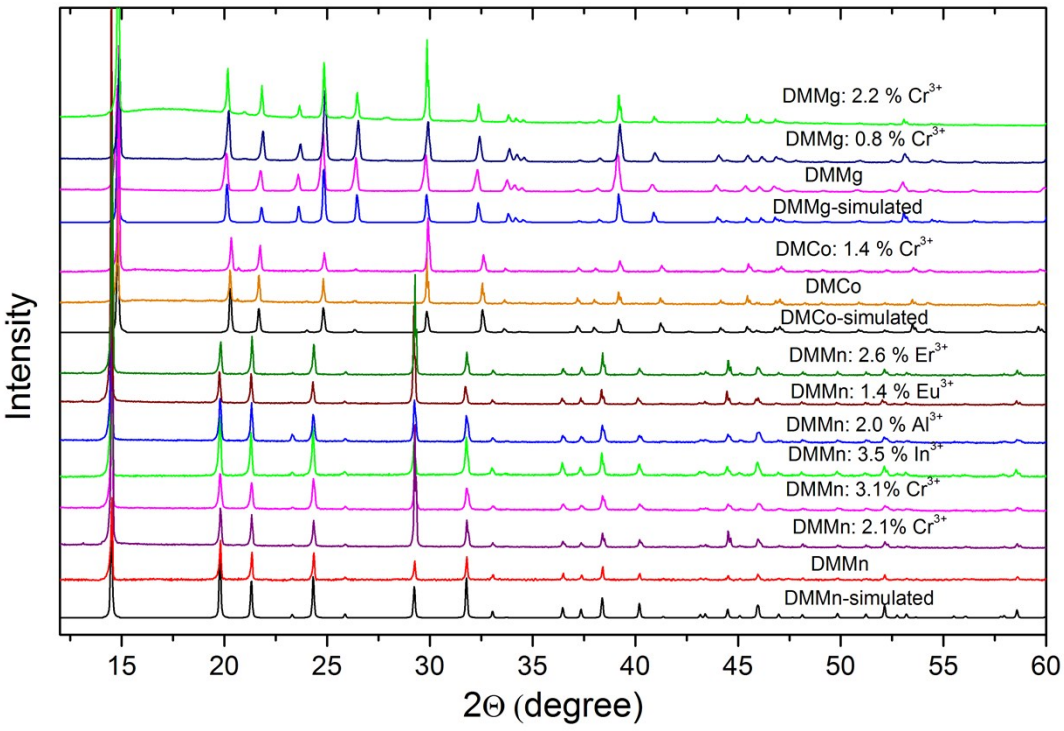

Figure S1. Powder XRD patterns for the as-prepared bulk samples and the simulated ones based on the room-temperature single crystal structures.

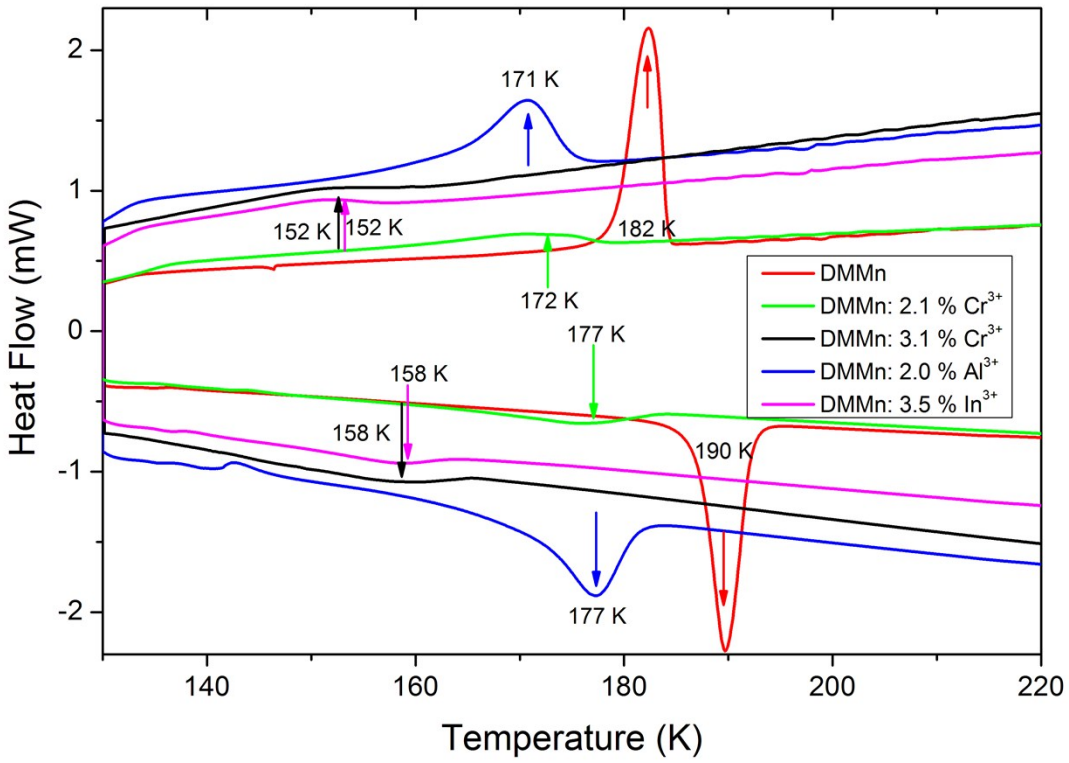

Figure S2. DSC traces for the studied DMMn samples (pure and doped with Cr^{3+}, Al^{3+} and In^{3+}) in heating and cooling modes.

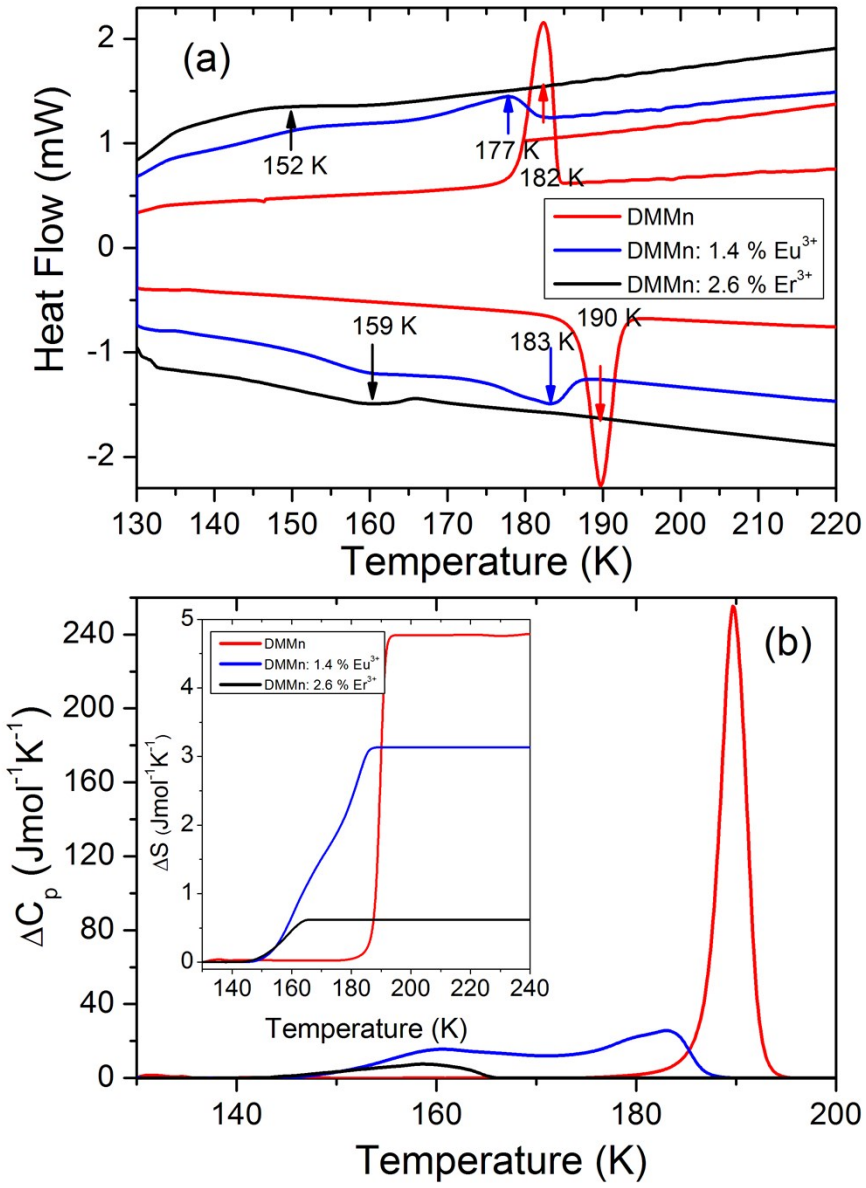

Figure S3. (a) DSC traces in heating and cooling modes and (b) the change in heat capacity of DMM, DMMn: 1.4 % Eu^{3+} and DMMn: 2.6 % Er^{3+} samples measured in heating mode. The inset shows the change in entropy related to the phase transitions.

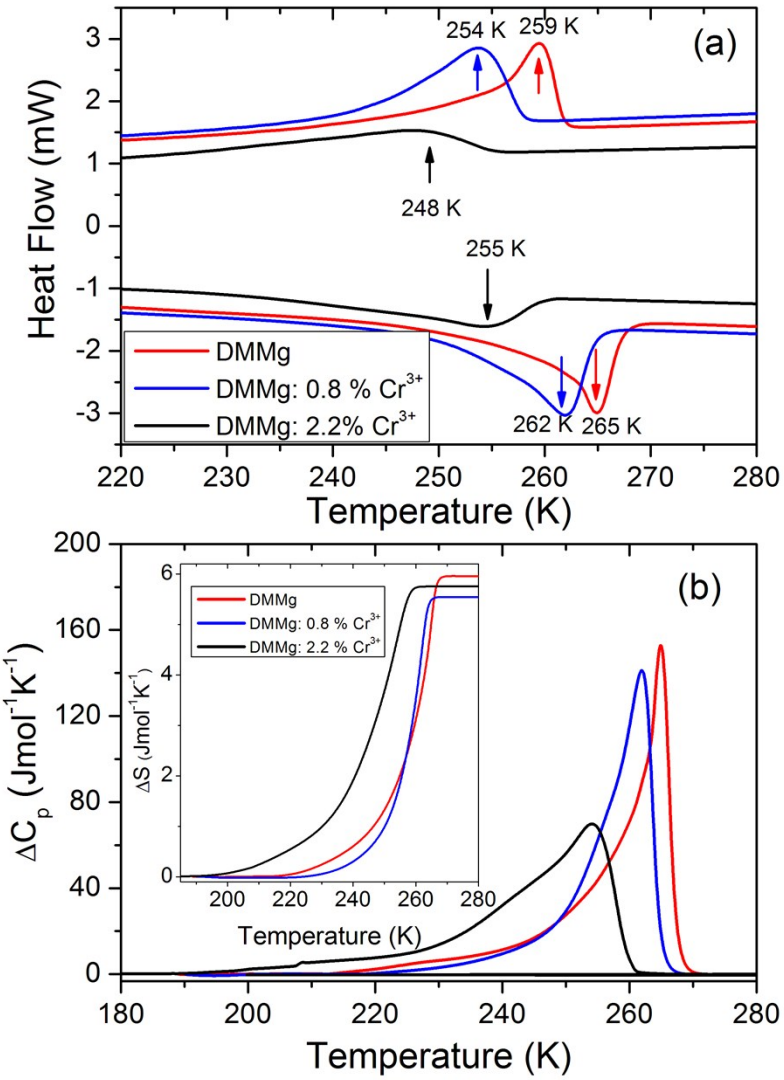

Figure S4. (a) DSC traces in heating and cooling modes and (b) the change in heat capacity of DMMg, DMMg: 0.8 % Cr^{3+} and DMMg: 2.2 % Cr^{3+} samples measured in heating mode. The inset shows the change in entropy related to the phase transitions.

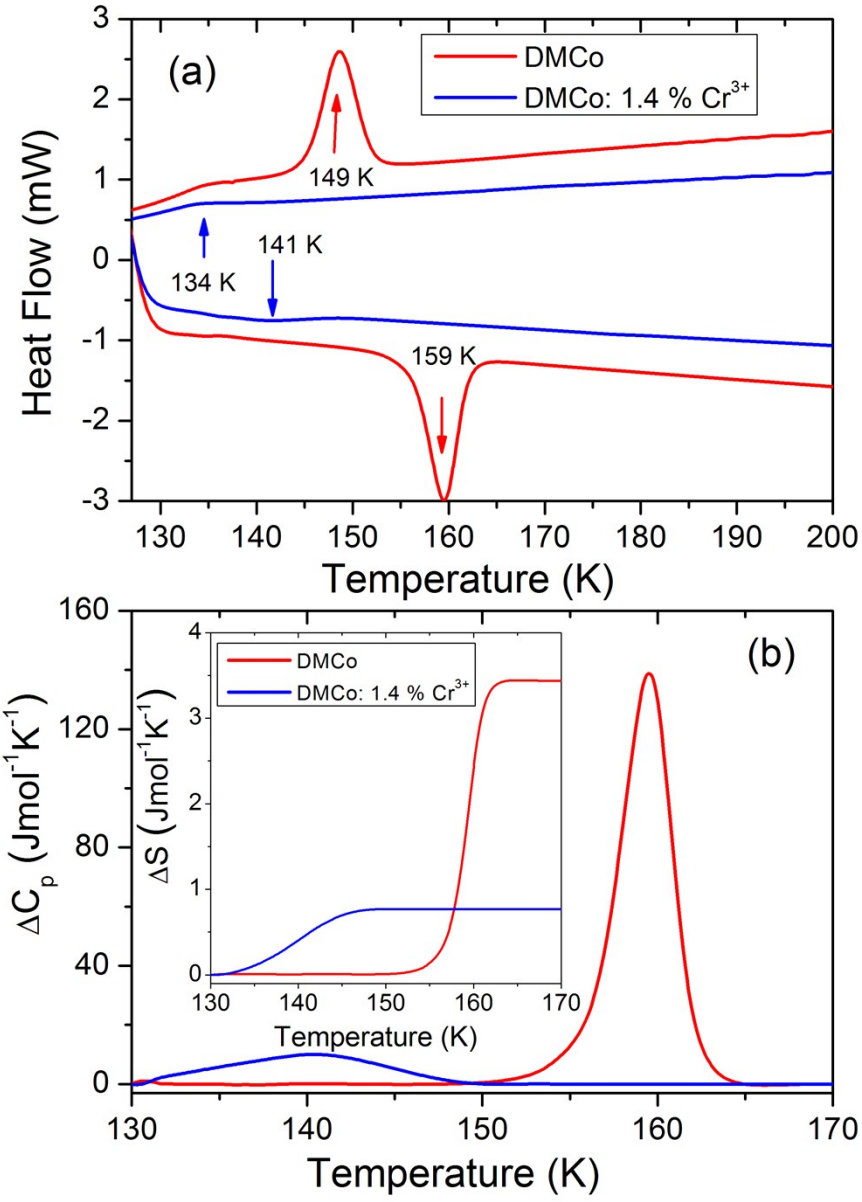

Figure S5. (a) DSC traces in heating and cooling modes and (b) the change in heat capacity of DMCo and DMCo: 1.4 % Cr^{3+} samples measured in heating mode. The inset shows the change in entropy related to the phase transitions.

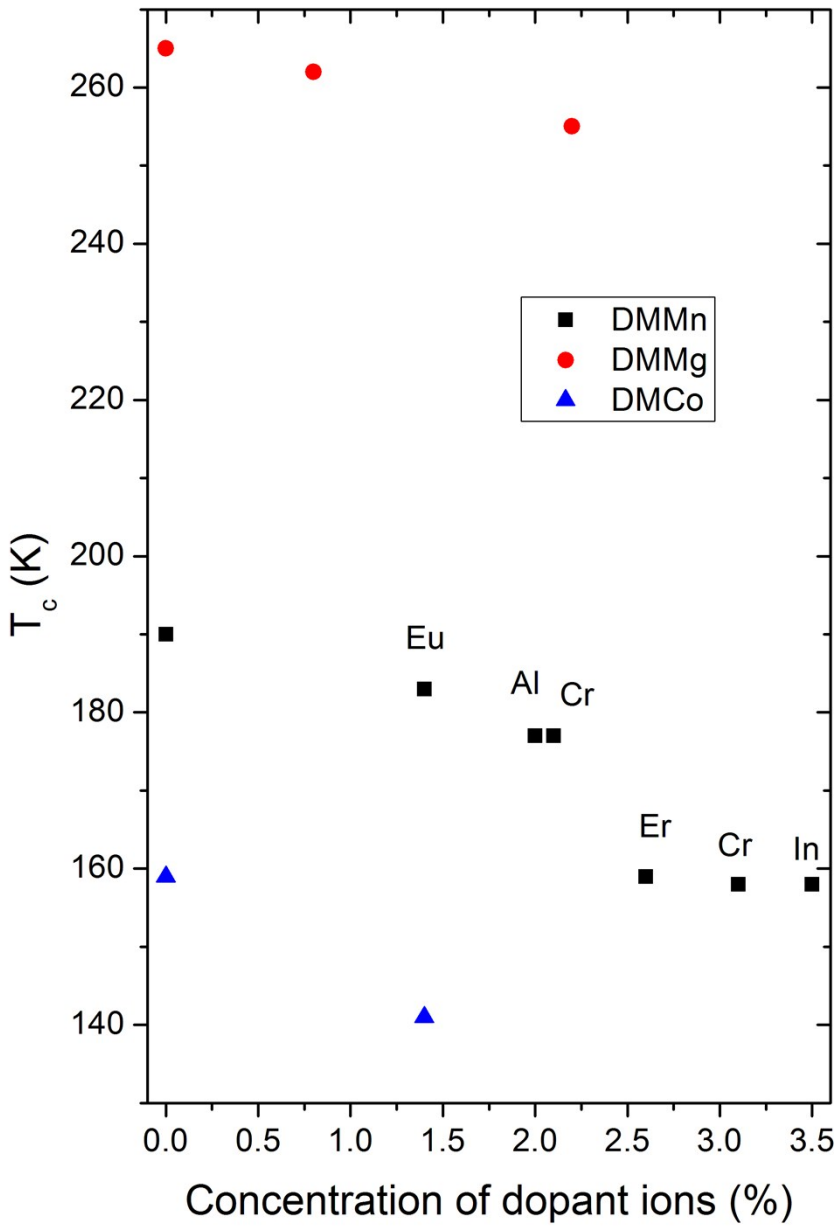

Figure S6. Dependence of the phase transition temperature T_c on concentration of the dopant ions in DMMn, DMCo and DMMg.

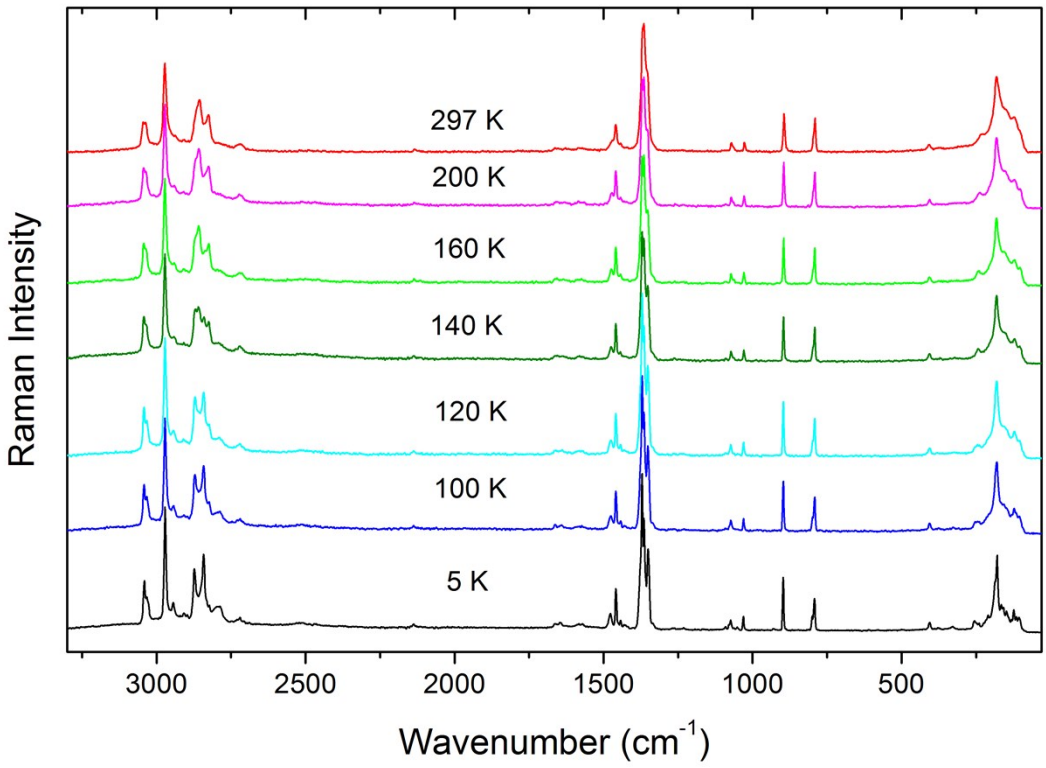

Figure S7. Raman spectra of DMMn: 3.1% Cr^{3+} recorded at various temperatures corresponding to the whole spectral range.

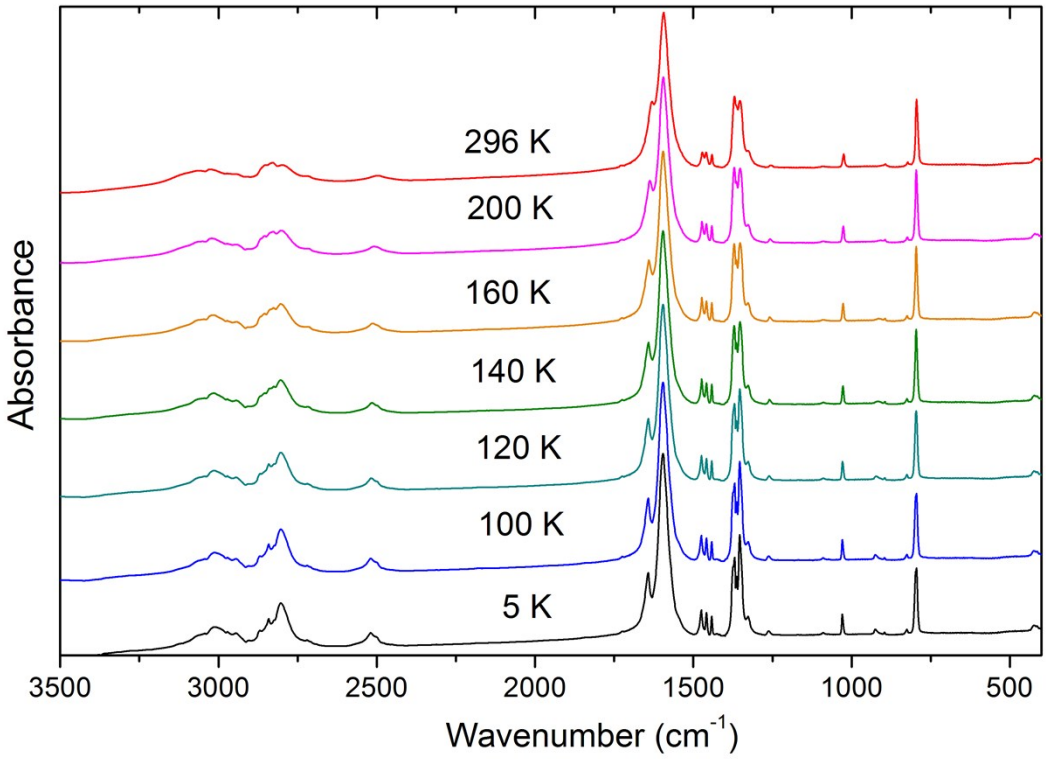

Figure S8. IR spectra of DMMn: 3.1% Cr^{3+} recorded at various temperatures corresponding to the spectral range 3500-400 cm^{-1}.

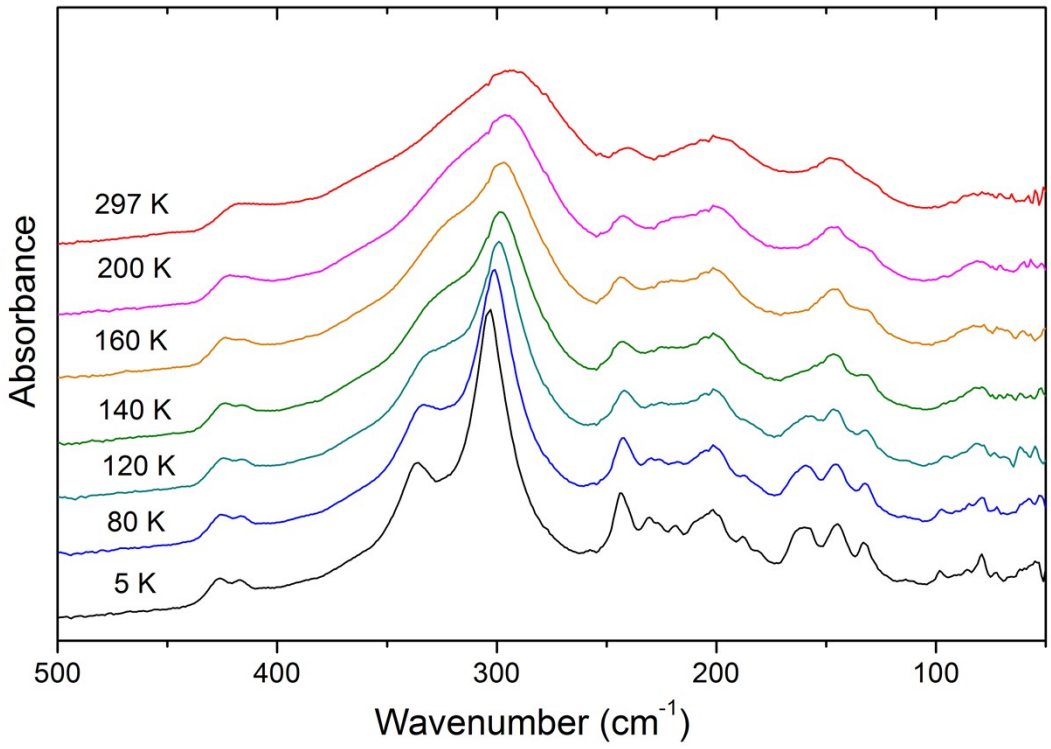

Figure S9. IR spectra of DMMn: 3.1% Cr^{3+} recorded at various temperatures corresponding to the spectral range 500-50 cm^{-1}.

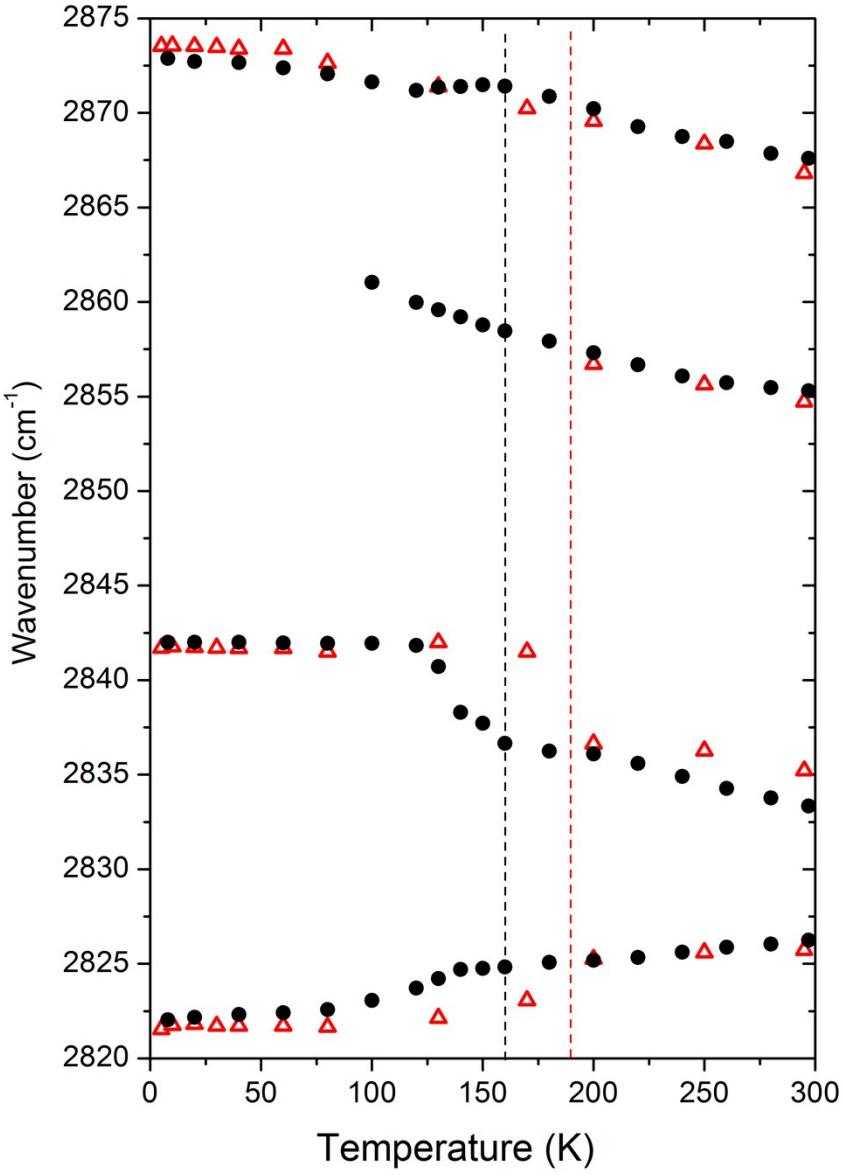

Figure S10. Temperature evolution of Raman frequencies of DMMn: 3.1% Cr^{3+} (circles) and DMMn (triangles) from the 2820-2875 cm^{-1} range. Vertical lines indicate the phase transition temperatures for undoped DMMn (red) and DMMn: 3.1 Cr^{3+} (black).

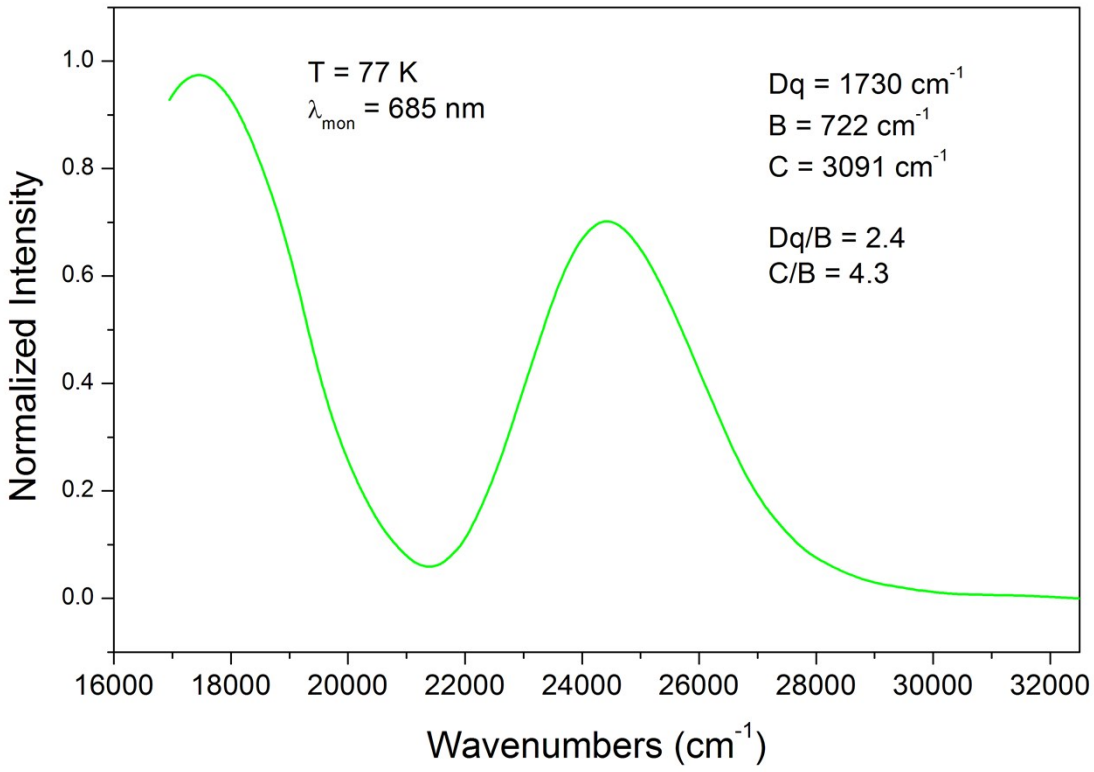

Figure S11. Excitation spectrum of DMMn: 3.1% Cr^{3+} recorded at 77 K with crystal field parameter and Racah parameters derived from the spectrum maxima.. Monitored wavelength was 685 nm.

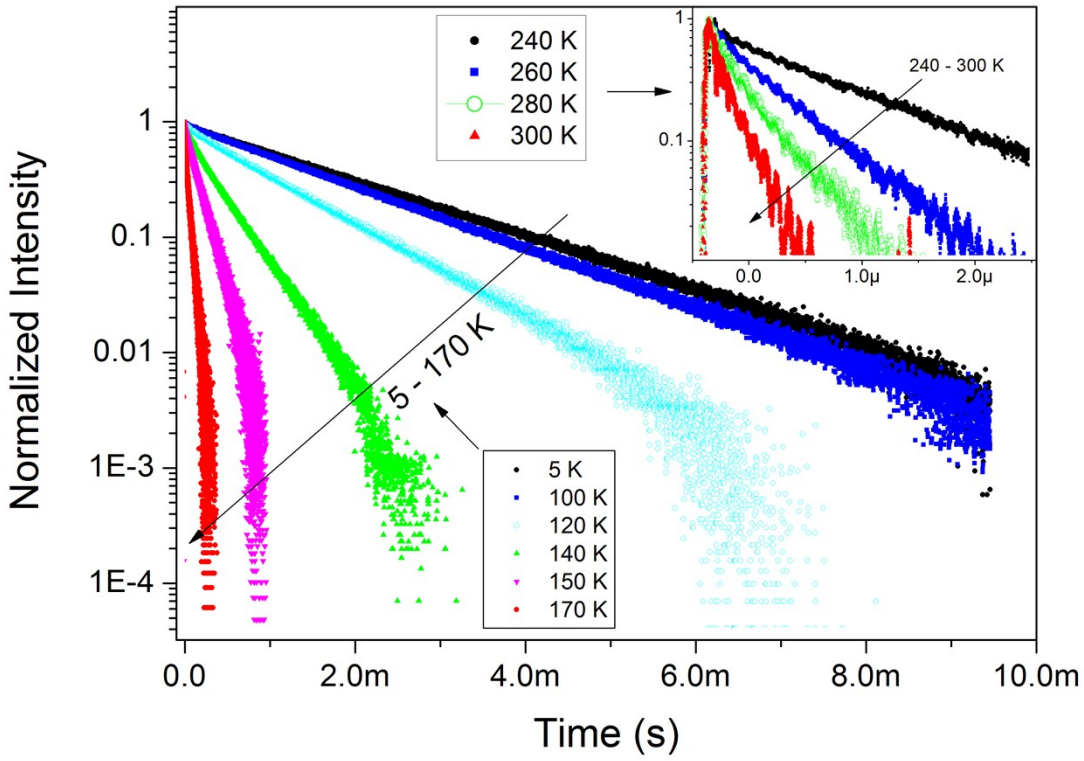

Figure S12. Emission decay profiles recorded at 5 – 220 K (inset: 240 – 300 K). Monitored wavenumber was at 14288 cm^{-1}.

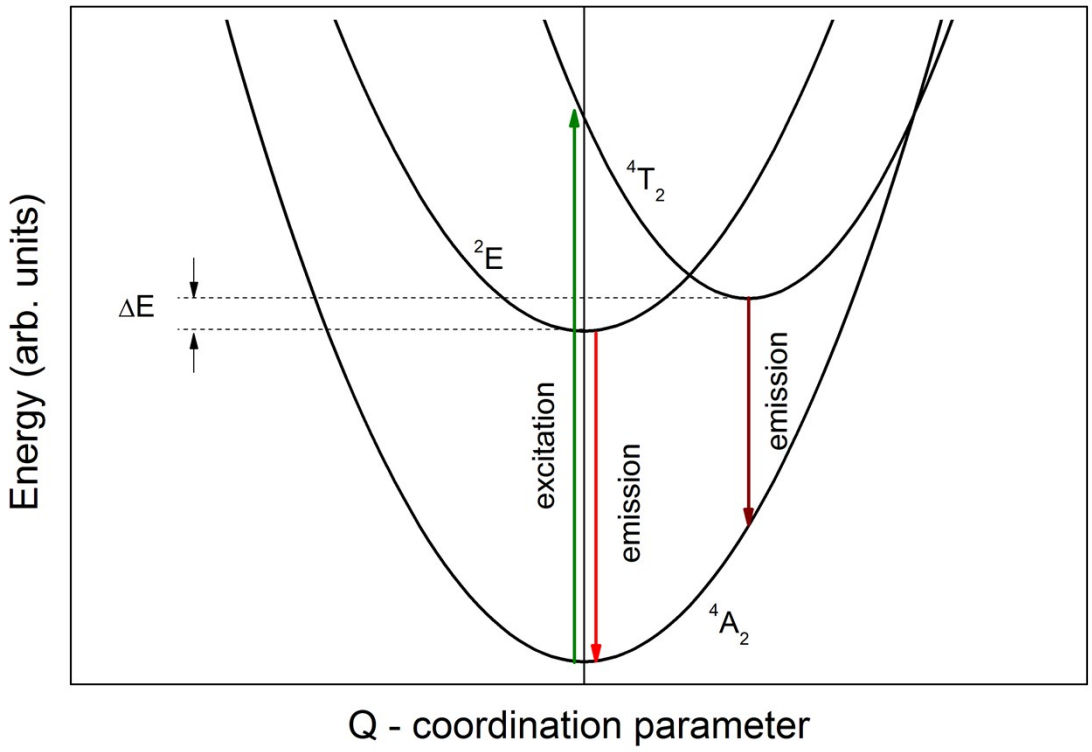

Figure S13. Single configurational coordinate model for Cr^{3+} in intermediate ligand field.

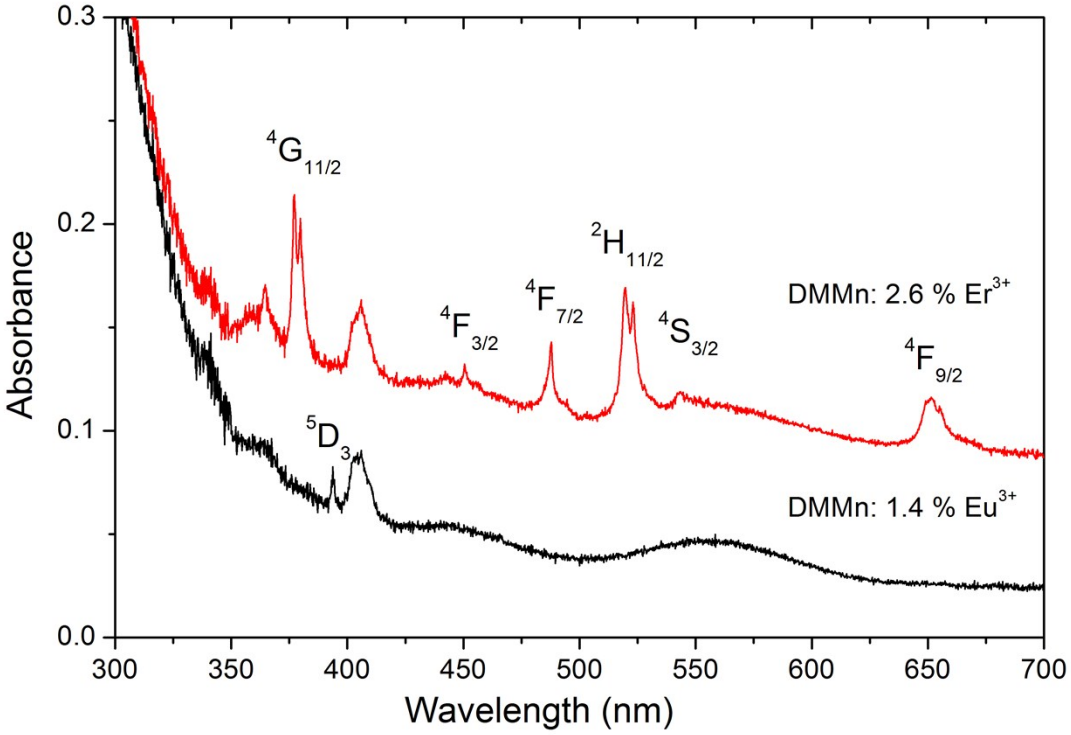

Figure S14. Room-temperature absorption spectra of DMMn: 2.6 % Er^{3+} and 1.4 % Eu^{3+}.